Fifth International Conference on Advanced COmputational Methods in ENgineering (ACOMEN 2011)
Liège, Belgium, 14-17 November 2011

Imposing periodic boundary condition on arbitrary meshes by polynomial interpolation

V.-D. Nguyen[1]*, E. Béchet[1], C. Geuzaine[2] and L. Noels[1]

[1] Department of Aerospace and Mechanical Engineering, University of Liège
Chemin des Chevreuils 1, B-4000 Liège, Belgium

[2] Department of Electrical Engineering and Computer Science, University of Liège
B28 P32, B-4000 Liège, Belgium

e-mails: {*VanDung.Nguyen, Eric.Bechet, CGeuzaine, L.Noels*}*@ulg.ac.be*

Abstract

In order to predict the effective properties of heterogeneous materials using the finite element approach, a boundary value problem (BVP) may be defined on a representative volume element (RVE) with appropriate boundary conditions, among which periodic boundary condition is the most efficient in terms of convergence rate. The classical method to impose the periodic boundary condition requires identical meshes on opposite RVE boundaries. This condition is not always easy to satisfy for arbitrary meshes. This work develops a new method based on polynomial interpolation that avoids the need of the identical mesh condition on opposite RVE boundaries.

1 Introduction

In the computational homogenization analysis, the effective properties of heterogeneous materials are obtained by solving the boundary value problem (BVP) which is defined as a representative volume element (RVE) with an appropriate boundary condition. Among classical boundary conditions proposed, the periodic boundary condition (PBC) is the most efficient with respect to convergence when the RVE size increases [1]. This conclusion also holds if the micro-structure does not possess geometrical periodicity [1, 2, 3]. Because of its efficiency, this work takes an interest in applying the PBC on arbitrary meshes.

To apply the PBC, the classical method consists in enforcing the same value for degrees of freedom of matching nodes on two opposite RVE sides. Thus, it requires a periodic mesh, which has the same mesh distribution on two opposite parts of the RVE boundary. In a more general setting, the conformity of mesh distributions on opposite boundaries of RVE cannot always be guaranteed, leading to a non-periodic mesh. For instance, in studies analyzing real micro-structures where the mesh is obtained by converting the finite element model from a micro-structure image processing [4], the mesh is generally non-periodic. Thus it is necessary to find another method which does not need a periodic mesh in order to apply the PBC. For this purpose, Larsson et al. [3] developed a weak enforcement of the PBC by introducing independently the finite element discretization of traction boundary and by allowing for the transition between the strongest form (PBC) to the weakest form (Neumann condition). Tyrus et al. [5] implemented the PBC for periodic composite materials, for arbitrary non-periodic mesh by enforcing a linear displacement field at intersection of fibers and RVE sides and a cubic displacement field at intersection of matrix and RVE sides. This method is restricted to a 2D-RVE where the unidirectional composite fibers are located solely at the corners of the 2D-RVE.

*PhD Candidate at the University of Liège, Department of Aerospace and Mechanical Engineering, CM3.

In this work, a method based on polynomial interpolation is proposed to apply the PBC to the RVE in a general way, with a view towards the characterization of micro-structured materials directly modeled from imaging processing, for which the mesh cannot be controlled. The idea of a polynomial interpolation given by Tyrus et al. [5] is generalized to be suitable for general mesh designs (periodic or non-periodic) in the 2-dimensional and 3-dimensional cases with periodic or random materials. In this new method, the displacement field of two opposite RVE sides is interpolated by appropriate functions, which are linear combinations of some shape functions considered as user parameters. The degrees of freedom of two opposite RVE sides are then substituted by the coefficients of these shape functions. This method allows to enforce strongly the PBC, without requirement of periodic mesh, from the "weakest constraint" (linear displacement boundary condition) corresponding to the polynomial order 1 to the "strongest constraint" (PBC) corresponding to the infinite polynomial order. Although this last case is theoretical, it can be approximated by using an interpolated function of high degree. The proposed method is shown to be easy to implement, and allows extracting effective material properties of a heterogeneous structures using a RVE of reduced size, for periodic and non-periodic structures.

2 Periodic boundary condition enforcement by polynomial interpolation

The microscopic problem is defined on a RVE of domain V, as following

$$\int_V \boldsymbol{\sigma} : \delta\boldsymbol{\varepsilon}\, dV = 0\,, \tag{1}$$

where $\boldsymbol{\sigma}$ and $\boldsymbol{\varepsilon}$ are the stress and strain tensor at the micro-scale. Many types of the boundary condition can be considered such as the linear displacement, constant traction and PBC. In this work, because of its efficiency, the PBC is used as following:

$$\boldsymbol{u}^+ - \boldsymbol{u}^- = \bar{\boldsymbol{\varepsilon}}.(\boldsymbol{x}^+ - \boldsymbol{x}^-)\,, \tag{2}$$

where $\boldsymbol{u}$ is the displacement vector, the notations $+$ and $-$ are the node indices which are associated with two opposite parts of the RVE boundary. This boundary condition depends on the macroscopic deformation tensor $\bar{\boldsymbol{\varepsilon}}$ which allows the micro-macro transition.

For periodic meshes, the existence of matching nodes on opposite faces of the RVE boundary allows to impose directly the PBC. However, for arbitrary meshes, a new approach should be considered. In this work it is proposed to develop a method based on the polynomial interpolation. The idea of this method is that the displacement field on the RVE boundary can be interpolated by appropriate functions $\mathbb{S}$ whose forms are known, and such that (2) is satisfied. Because of its simplicity, a polynomial form is used as interpolation. In general, it is possible to express the general form of an interpolation by

$$\boldsymbol{u}(\boldsymbol{s}) = \mathbb{S}(\boldsymbol{s}) = \sum_{i=0}^{n} \mathbb{N}_i(\boldsymbol{s})\boldsymbol{a}_i\,, \tag{3}$$

where each function $\mathbb{N}_i(\boldsymbol{s})$, with $i = 0, .., n$, only depends on the spatial variable $\boldsymbol{s}$, and where each variable $\boldsymbol{a}_i$, $i = 0, .., n$ is an independent first order tensor of degrees of freedom introduced in the finite element calculation.

In this work, the negative part of the RVE boundary is interpolated with the polynomial form $\mathbb{S}(\boldsymbol{s})$. As for the PBC, equation (2) should be satisfied, the displacement field on the positive part should also be expressed in terms of $\mathbb{S}(\boldsymbol{s})$, leading to

$$\boldsymbol{u}_-(\boldsymbol{s}) = \mathbb{S}(\boldsymbol{s})\,, \text{ and} \tag{4}$$

$$\boldsymbol{u}_+(\boldsymbol{s}) = \mathbb{S}(\boldsymbol{s}) + \bar{\boldsymbol{\varepsilon}}.(\boldsymbol{x}^+ - \boldsymbol{x}^-)\,, \tag{5}$$

where the term $\bar{\boldsymbol{\varepsilon}}(\boldsymbol{x}^+ - \boldsymbol{x}^-)$ depends on the macroscopic strain tensor and the RVE dimension.

For imposing (4)(5) in the finite element framework, the nodal displacements on negative part of the RVE boundary are given by

$$\boldsymbol{u}_{-} \;=\; \tilde{\mathbb{N}}\tilde{\boldsymbol{q}}\,, \tag{6}$$

where $\tilde{\mathbb{N}}$ is the interpolation shape functions matrix and $\tilde{\boldsymbol{q}}$ is the independent variables vector.

Applying the PBC (2) yields the nodal displacement interpolation on the positive edge:

$$\boldsymbol{u}_{+} \;=\; \tilde{\mathbb{N}}\tilde{\boldsymbol{q}} + \bar{\boldsymbol{\varepsilon}}(\boldsymbol{x}^{+} - \boldsymbol{x}^{-}) \tag{7}$$

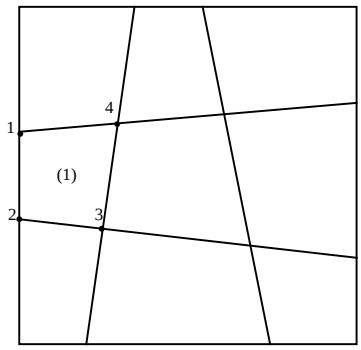

Figure 1: Simple mesh for illustration purpose.

To illustrate the finite element implementation of the polynomial interpolation, the simple 2D-mesh of Fig. 1 is considered. The constraints will be enforced for element 1 defined from the 4 nodes (1,2,3,4). In the finite element interpolation formulation, the displacement field inside this element reads

$$\boldsymbol{u}_e(x,y) \;=\; N_1(x,y)\boldsymbol{u}_1 + N_2(x,y)\boldsymbol{u}_2 + N_3(x,y)\boldsymbol{u}_3 + N_4(x,y)\boldsymbol{u}_4 = \mathbb{N}_e\boldsymbol{q}_e, \;\text{ with} \tag{8}$$

$$\boldsymbol{q}_e^T \;=\; [\;\boldsymbol{u}_1^T \quad \boldsymbol{u}_2^T \quad \boldsymbol{u}_3^T \quad \boldsymbol{u}_4^T\;]\,. \tag{9}$$

As nodes 1 and 2 of this element lie on the boundary, assuming on its negative part, the polynomial interpolation implies

$$\boldsymbol{u}_1 \;=\; \mathbb{N}_1\tilde{\boldsymbol{q}}\,, \text{ and} \tag{10}$$

$$\boldsymbol{u}_2 \;=\; \mathbb{N}_2\tilde{\boldsymbol{q}}\,. \tag{11}$$

In case they lie on the positive part of the boundary, these last two relations become :

$$\boldsymbol{u}_1 \;=\; \mathbb{N}_1\tilde{\boldsymbol{q}} + \bar{\boldsymbol{\varepsilon}}(\boldsymbol{x}^{+} - \boldsymbol{x}^{-})\,, \text{ and} \tag{12}$$

$$\boldsymbol{u}_2 \;=\; \mathbb{N}_2\tilde{\boldsymbol{q}} + \bar{\boldsymbol{\varepsilon}}(\boldsymbol{x}^{+} - \boldsymbol{x}^{-})\,. \tag{13}$$

Thus, the displacement field (9) of the element nodes can be restated as

$$\boldsymbol{q}_e = \begin{bmatrix} \boldsymbol{u}_1 \\ \boldsymbol{u}_2 \\ \boldsymbol{u}_3 \\ \boldsymbol{u}_4 \end{bmatrix} = \begin{bmatrix} \mathbb{N}_1\tilde{\boldsymbol{q}} + \langle \boldsymbol{g} \rangle \\ \mathbb{N}_2\tilde{\boldsymbol{q}} + \langle \boldsymbol{g} \rangle \\ \boldsymbol{u}_3 \\ \boldsymbol{u}_4 \end{bmatrix} = \mathbb{L}_e\tilde{\boldsymbol{q}}_e \;+ \tilde{\boldsymbol{g}}_e\,, \tag{14}$$

where $\tilde{\boldsymbol{q}}_e^T = [\boldsymbol{u}_3^T \quad \boldsymbol{u}_4^T \quad \tilde{\boldsymbol{q}}^T]$ is the new elementary vector of degrees of freedom, where $\mathbb{L}_e$ is the mapping matrix which allows transforming the element displacement vector $\boldsymbol{q}_e$ into the constraint displacement vector $\tilde{\boldsymbol{q}}_e$, where $\langle \boldsymbol{g} \rangle$ is the contribution of $\bar{\boldsymbol{\varepsilon}}(\boldsymbol{x}^{+} - \boldsymbol{x}^{-})$ for nodes lying on the positive boundary part and is equal to zero for nodes lying on the negative boundary part, and where $\tilde{\boldsymbol{g}}_e$ is the elementary vector related to $\langle \boldsymbol{g} \rangle$.

The finite element equation without constraints, written in terms of the elementary values, reads

$$\sum_e \left(\boldsymbol{\delta q}_e^T \boldsymbol{K}_e \boldsymbol{q}_e\right) - \sum_e \left(\boldsymbol{\delta q}_e^T \boldsymbol{F}_e\right) = 0\,, \tag{15}$$

where $\delta \boldsymbol{q}_e$ is the arbitrary virtual displacement, where $\boldsymbol{K}_e$ is the elementary stiffness matrix and where $\boldsymbol{F}_e$ is the elementary force vector. According to Eq. (14), the virtual displacement becomes:

$$\boldsymbol{\delta q}_e = \mathbb{L}_e \boldsymbol{\delta \tilde{q}}_e\,, \tag{16}$$

and substituting this relation into (15), the new finite element formulation of non-constrained displacement $\tilde{q}_e$ reads

$$\sum_e \left(\boldsymbol{\delta \tilde{q}}_e^T \mathbb{L}_e^T \boldsymbol{K}_e \mathbb{L}_e \boldsymbol{\tilde{q}}_e\right) - \sum_e \left(\boldsymbol{\delta \tilde{q}}_e^T \mathbb{L}_e^T \boldsymbol{F}_e - \boldsymbol{\delta \tilde{q}}_e^T \mathbb{L}_e^T \boldsymbol{K}_e \boldsymbol{\tilde{g}}_e\right) = 0 \tag{17}$$

or

$$\sum_e \boldsymbol{\delta \tilde{q}}_e^T \left(\boldsymbol{\tilde{K}}_e \boldsymbol{\tilde{q}}_e - \boldsymbol{\tilde{F}}_e\right) = 0\,, \tag{18}$$

where $\boldsymbol{\tilde{K}}_e = \mathbb{L}_e^T \boldsymbol{K}_e \mathbb{L}_e$ is the modified elementary stiffness matrix and where $\boldsymbol{\tilde{F}}_e = \mathbb{L}_e^T \left(\boldsymbol{F}_e - \boldsymbol{K}_e \boldsymbol{\tilde{g}}_e\right)$ is the modified elementary force vector.

Equation (18) defines the implementation of the polynomial interpolation. In theory, the independent variables $\boldsymbol{\tilde{q}}$ can be chosen independently of the existing nodal displacements on the RVE boundary.

3 Numerical applications

The material used in this work is elastic (Young modulus $E = 70GPa$ and Poisson ration $\nu = 0.3$).

3.1 Bidimensional application

For bidimensional problems, two formulations are suggested to interpolate the displacement field on the negative edge of RVE boundary: the Lagrange formulation and the cubic spline formulation. The calculation is investigated in the plane strain state ($\varepsilon_{zz} = \varepsilon_{xz} = \varepsilon_{yz} = 0$).

Lagrange formulation: The displacement field on the negative edge of the RVE boundary is approximated by the polynomial $\mathbb{S}$ of order n,

$$\mathbb{S}(s) = \sum_{i=0}^{n} \boldsymbol{a}_i s^i\,. \tag{19}$$

This polynomial form requests $n+1$ independent variables $\boldsymbol{a}_i$, with $i = 0, .., n$, defined from $n+1$ sampling displacements $\boldsymbol{u}_0, ..., \boldsymbol{u}_n$ evaluated at the sampling points $s_0, ..., s_n$. These sampling points can coincide to the mesh nodes or not. The polynomial $\mathbb{S}$ can thus be reformulated as

$$\boldsymbol{u} = \mathbb{S}(s) = \sum_{i=0}^{n} l_i(s) \boldsymbol{u}_i\,, \tag{20}$$

where l_i is the Lagrange polynomial associated to the sampling couple $(s_i, \boldsymbol{u}_i)$, and given by

$$l_i(s) = \prod_{j=0, j\neq i}^{n} \frac{s - s_j}{s_i - s_j}\,. \tag{21}$$

The function l_i satisfies $l_i(s_j) = \delta_{ij}$ and the norm

$$\sum_{i=0}^{n} l_i(s) = 1\,. \tag{22}$$

Particularly, if $n = 1$, the linear displacement boundary condition is recovered. In the matrix form, the equation (20) is rewritten as

$$\boldsymbol{u}(s) \quad = \quad \tilde{\mathbb{N}}(s)\tilde{\boldsymbol{q}}\,, \tag{23}$$

where $\tilde{\boldsymbol{q}}^T = [\boldsymbol{u}_0^T ... \boldsymbol{u}_n^T]$ is the independent variables vector and where $\tilde{\mathbb{N}}$ is the interpolation shape functions matrix.

Cubic spline formulation: For this formulation, an edge is divided into N segments $[(s_{i-1}, \boldsymbol{u}_{i-1}) \quad (s_i, \boldsymbol{u}_i)]$ defined from the $n+1$ sampling couples $(s_0, \boldsymbol{u}_0), ..., (s_N, \boldsymbol{u}_N)$. At the extremities of each segment, two slope vectors $\boldsymbol{\theta}_{i-1}, \boldsymbol{\theta}_i$ are also defined, so the displacement field in each segment can be interpolated using the Hermite polynomials of order 3:

$$H_1(\xi) \quad = \quad 1 - 3\xi^2 + 2\xi^3\,, \tag{24}$$
$$H_2(\xi) \quad = \quad d(\xi - 2\xi^2 + \xi^3)\,, \tag{25}$$
$$H_3(\xi) \quad = \quad 3\xi^2 - 2\xi^3\,, \tag{26}$$
$$H_4(\xi) \quad = \quad d(-\xi^2 + \xi^3)\,, \tag{27}$$

where $\xi(s) = \frac{s - s_{i-1}}{s_i - s_{i-1}}$ and where $d = s_i - s_{i-1}$ is the segment length. Therefore, the displacement field can be interpolated on this segment from

$$\boldsymbol{u}(s) = H_1(\xi(s))\boldsymbol{u}_{i-1} + H_2(\xi(s))\boldsymbol{\theta}_{i-1} + H_3(\xi(s))\boldsymbol{u}_i + H_4(\xi(s))\boldsymbol{\theta}_i\,. \tag{28}$$

Equation (28) can be rewritten in the matrix form:

$$\boldsymbol{u}(s) \quad = \quad \tilde{\mathbb{N}}(\xi)\tilde{\boldsymbol{q}}\,, \tag{29}$$

where $\tilde{\boldsymbol{q}}^T = [\boldsymbol{u}_0^T \boldsymbol{\theta}_0^T ... \boldsymbol{u}_N^T \boldsymbol{\theta}_N^T]$ is the independent variables vector and $\tilde{\mathbb{N}}$ is the interpolation shape functions matrix.

By using the finite element implementation presented in section 2, two formulations above are used to enforce the PBC for both periodic mesh and non-periodic mesh, see Fig. 2.

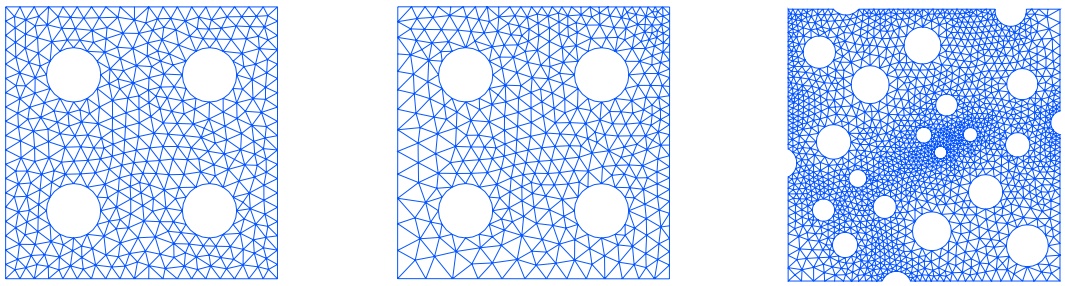

(a) (b) (c)

Figure 2: RVEs used in the method analysis: (a) Periodic mesh, (b) Non-periodic mesh generated from periodic hole distribution, the void fraction is 0.1257 and (c) Non- periodic mesh generated from a random hole distribution, the void fraction is 0.1657

The polynomial interpolation implementation is equivalent to introducing constraints in the system, with the two extreme cases: The PBC is equivalent to the less constrained case (polynomial interpolation with infinity order) and linear displacement boundary condition is equivalent to the most constrained case (polynomial interpolation with order 1). Thus, the results given by the polynomial interpolation method must converge to the effective modulus value given by classical PBC implementation when the number of independant variables added to the system (size of the vector $\tilde{\boldsymbol{q}}$ in Eqs. (23)(29)) increases as presented in Fig. 3. Thes results are compared with the result given by the constraint elimination method of the periodic mesh (presented in [6]).

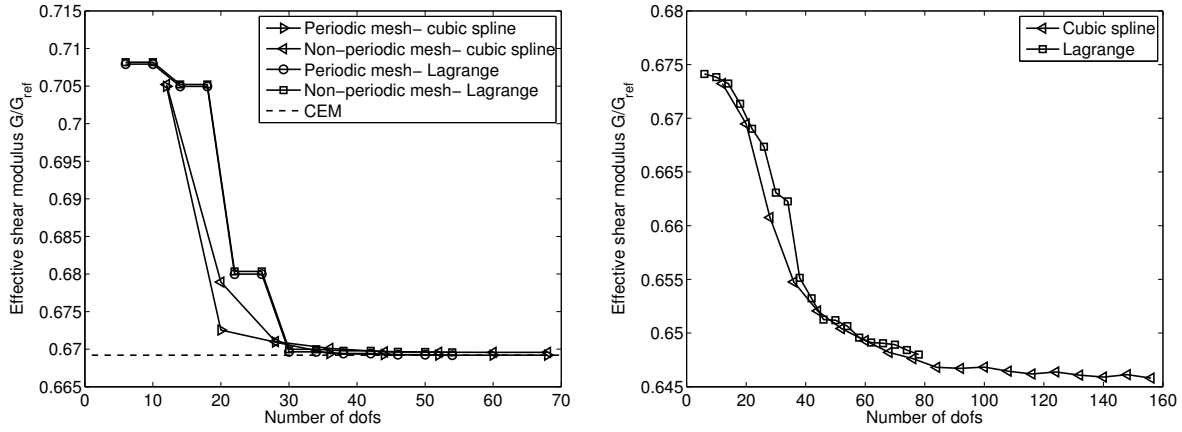

(a) (b)

Figure 3: Influence of polynomial interpolation parameters on the in-plane effective shear modulus in terms of the number of degrees of freedom of the boundary displacement field: (a) Periodic structure and (b) Non-periodic structure. Results with the periodic structures are compared to the result given by constraint elimination method computed with periodic mesh (noted as CEM).

3.2 Tridimensional application

For 3-dimensional problems, many surface interpolation formulations can be used, such as B-splines, to interpolate the displacement field on the boundary surfaces. In this work, in order to illustrate the efficiency of the method in the 3-dimensional case, a simple bi-linear patch Coons formulation is considered, but more evolved formulations can directly be derived. The displacement field on the boundary edges of the RVE is interpolated using the Lagrange or cubic spline formulation presented in the previous section.

A RVE with void fraction 0.41 is studied. Cavities are cylindrical and unidirectional. The generated mesh is non-periodic and is shown in Fig.4a. The macro-strain tensor applied to the RVE implies different loading modes:

$$\bar{\boldsymbol{\epsilon}} = \begin{bmatrix} 0.01 & 0.05 & -0.05 \\ 0.05 & 0.01 & 0.05 \\ -0.05 & 0.05 & -0.01 \end{bmatrix} . \tag{30}$$

Two ways of enforcing the PBC are studied. First, the Lagrange interpolation method is used with a polynomial order of 15 for all edges of the RVE. Second, the cubic spline interpolation is implemented with 10 segments on each edge of RVE. The displacement of internal points on boundary surface is interpolated by a bilinear Coons patch in both cases.

The average macro-stress tensor obtained with the Lagrange interpolation is given by

$$\bar{\sigma}_{lagrange} = \begin{bmatrix} 281.583 & 92.392 & 121.181 \\ 92.392 & 270.111 & -115.835 \\ 121.181 & -115.835 & -247.78 \end{bmatrix} \text{MPa}\,, \tag{31}$$

while the one obtained using the cubic spline interpolation is given by

$$\bar{\sigma}_{spline} = \begin{bmatrix} 281.399 & 91.9833 & 121.239 \\ 91.983 & 268.85 & -115.614 \\ 121.239 & -115.614 & -248.214 \end{bmatrix} \text{MPa}\,. \tag{32}$$

The resulting deformations of the RVE are presented in Figs. 4b,c for the Lagrange interpolation and the cubic spline interpolation respectively. This figure shows that the RVE deformation forms obtained with the two approaches are in good agreement. This section shows that the polynomial interpolation method can be used to apply the periodic boundary condition on a 3D-RVE in a straightforward way.

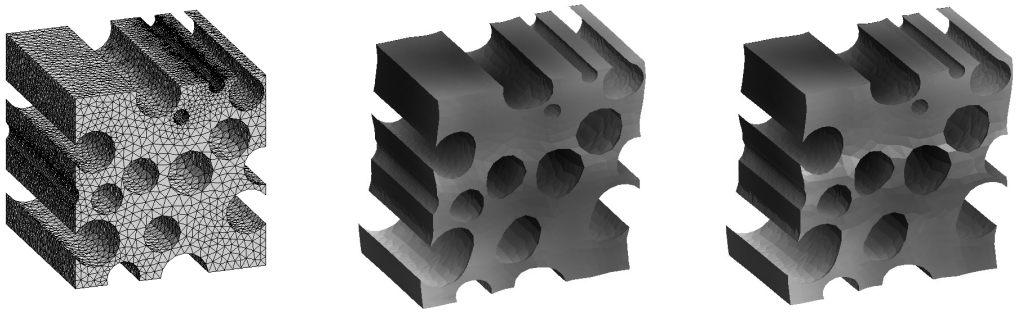

(a) (b) (c)

Figure 4: Deformation of the RVE with the periodic boundary condition enforced with polynomial interpolation: (a) 3D mesh, (b) Deformation of the RVE with the Lagrange interpolation and (c) Deformation of RVE with cubic spline interpolation.

3.3 Validation

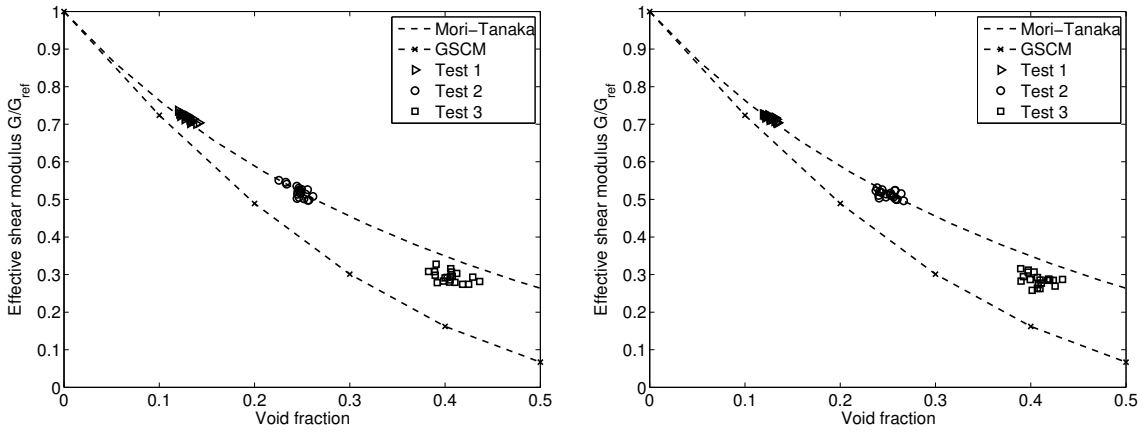

(a) (b)

Figure 5: Comparison of the in-plane effective shear modulus obtained from the finite element model using (a) the spline interpolation and (b) the Lagrange interpolation approaches with those predicted by the different theoretical methods (general self-consistent method GSCM and Mori-Tanaka method). The finite element models consider a random micro-structure. Markers correspond to realizations results.

Effective material properties extracted from the RVEs with the enforcement of the periodic boundary condition from the polynomial interpolation are compared with those predicted by the Mori-Tanaka [7] and GSCM [8] approaches. For the random micro-structures, for each RVE size, series of realizations are considered to estimate the effective modulus [2]. In this application, three series with average void fraction of 0.128, 0.25, 0.41, and denoted by Test 1, Test 2, Test 3 respectively, are considered. The exact void fraction on each RVE cannot be exactly the one of the heterogeneous material. This motivates the use of 20 realizations for each Test series.

Figs. 5 present the extracted in-plane effective shear modulus obtained with the periodic boundary condition enforced by the cubic spline and Lagrange interpolations. It is found that the dispersion in the extracted properties is more important for higher void fractions. For small void fractions (Test 1 and Test 2), the numerical results are very close to those predicted by Mori-Tanaka approach. The GSCM under-predicts the present numerical results. Results with higher void fraction (Test 3) lie in the region limited by those given by the Mori-Tanaka approach and by the GSCM.

As it is well known that the Mori-Tanaka approach provides a good estimation of the material properties for random micro-structures, this section demonstrates the accuracy of the implemented algorithm based on polynomial enforcement of the periodic boundary condition.

4 Conclusion

While the meshes generated for the periodic micro-structures are controllable, the meshes generated for the random micro-structures are not totally controlled. In the first case the periodic boundary condition can be apply by traditional constraint elimination method or by the newly proposed polynomial interpolation method, which allows validating our approach. In the second case, only the new method can be considered, which allows demonstrating its efficiency.

For a given RVE, the results always converge with the increase of the polynomial order and the polynomial interpolation was shown to provide accurate results in comparison to those given by the constraint elimination method and those given by some existing theoretical models as the Mori-Tanaka method and the GSCM. In all the cases, the method was demonstrated to be more accurate than the enforcement of linear displacement for boundary conditions, which is usually considered for random micro-structures. Moreover, the presented formulation does not induce an increase in the computational expenses as the number of degree of freedom is not increased.

Acknowledgment

Les recherches ont été financées grâce à la subvention "Actions de recherche concertées ARC 09/14-02 BRIDGING - From imaging to geometrical modelling of complex micro structured materials: Bridging computational engineering and material science" de la Direction générale de l'Enseignement non obligatoire de la Recherche scientifique, Direction de la Recherche scientifique, Communauté française de Belgique, et octroyées par l'Académie Universitaire Wallonie-Europe.

References

[1] Kenjiro Terada, Muneo Hori, Takashi Kyoya, and Noboru Kikuchi. Simulation of the multi-scale convergence in computational homogenization approaches. *International Journal of Solids and Structures*, 37(16):2285–2311, 2000.

[2] T. Kanit, S. Forest, I. Galliet, V. Mounoury, and D. Jeulin. Determination of the size of the representative volume element for random composites: statistical and numerical approach. *International Journal of Solids and Structures*, 40(13-14):3647–3679, 2003.

[3] F. Larsson, K. Runesson, S. Saroukhani, and R. Vafadari. Computational homogenization based on a weak format of micro-periodicity for rve-problems. *Computer Methods in Applied Mechanics and Engineering*, 200(1-4):11–26, 2011.

[4] G. Legrain, P. Cartraud, I. Perreard, and N. Moës. An x-fem and level set computational approach for image-based modelling: Application to homogenization. *Int. J. Numer. Meth. Engng.*, 2010.

[5] J. M. Tyrus, M. Gosz, and E. DeSantiago. A local finite element implementation for imposing periodic boundary conditions on composite micromechanical models. *International Journal of Solids and Structures*, 44(9):2972–2989, 2007.

[6] D. Peric, E. A. de Souza Neto, R. A. Feijóo, M. Partovi, and A. J. Carneiro Molina. On micro-to-macro transitions for multi-scale analysis of non-linear heterogeneous materials: unified variational basis and finite element implementation. *Int. J. Numer. Meth. Engng.*, 2010.

[7] T Mori and K Tanaka. Average stress in matrix and average elastic energy of materials with misfitting inclusions. *Acta Metallurgica*, 21(5):571 – 574, 1973.

[8] A. Pan'kov. Generalized self-consistent method: Modeling and computation of effective elastic properties of composites with composite or hollow inclusions. *Mechanics of Composite Materials*, 34:123–131, 1998. 10.1007/BF02256032.